Article:

Smith, AM, Singh, S and Ross, AB (2016) Fate of inorganic material during hydrothermal carbonisation of biomass: Influence of feedstock on combustion behaviour of hydrochar. Fuel, 169. pp. 135-145. ISSN 0016-2361

https://doi.org/10.1016/j.fuel.2015.12.006

Fate of inorganic material during hydrothermal carbonisation of biomass: influence of feedstock on combustion behaviour of hydrochar

Aidan M. Smith[a], Surjit Singh[a] and Andrew B. Ross[1a]

[a]Energy Research Institute, School of Chemical and Process Engineering, University of Leeds

Abstract

A series of high moisture content biomass have been processed by hydrothermal carbonisation (HTC) in a batch reactor at two temperatures (200 °C and 250 °C). The feedstocks processed include food waste, secondary sewage sludge, AD press cake, microalgae, macroalgae and a fibre derived from municipal derived wastes. In addition, three lignocellulosic biomass including miscanthus, willow and oak wood have been processed under identical conditions. The yields and properties of the resulting hydrochars including their HHV, CHNS, mineral content and ash fusibility properties have been determined and compared with their starting biomass. Typical char yields for lignocellulosic material range between 58-70 wt% at 200 °C and reduce to 40-46 wt% at 250 °C. The behaviour and mass balance is however very feedstock dependent and the higher lignin biomass produce higher yields of hydrochar. There is a significant upgrading of the energy density of the hydrochars with calculated HHV ranging from typically 24 $MJkg^{-1}$ at 200 °C to 28-31 $MJkg^{-1}$ at 250 °C for lignocellulosic material. The exception is for sewage sludge and AD press cake which result in a significant solubilisation of organic matter. A significant removal of alkali metals is observed and this in turn changes the ash chemistry upon combustion. This change in ash chemistry has been shown to change the ash melting behaviour and the hemisphere temperatures (oxidizing conditions) were seen to increase substantially. A number of predictive slagging and fouling indices have been used to evaluate the influence of the ash chemistry on the fuel combustion behaviour and this combined with the ash fusion testing has shown that HTC reduces the potential fouling and slagging in some of the resulting hydochars if combusted.

---

[1] Corresponding author: Email address: a.b.ross@leeds.ac.uk (A.B. Ross). Postal Address: Energy Research Institute, School of Chemical and Process Engineering, University of Leeds, LS2 9JT, UK

Keywords: biomass pre-treatment, hydrochar, ash, combustion, inorganic elements, fouling index

1. Introduction

Biomass is becoming an attractive energy resource as it offers benefits in terms of its potential sustainability and carbon neutrality. However when compared to solid fossil fuels such as coal, biomass suffers due its low bulk density, high moisture content, low calorific value and high hydrophillic nature. This combined with milling difficulties brought about through the fibrous nature of biomass means that the handling properties of raw biomass negatively influence the economies of biomass. This has prompted considerable interest in pre-treatment of biomass which may help overcome some of these limitations. One such process is torrefaction which has received increasing interest in recent years. Torrefaction is a thermal process that involves the heating of biomass between 250°C and 300°C in an inert atmosphere; driving out moisture and low calorific components to increase the fuels calorific value (Ibrahim et al., 2013). Torrefaction however requires a dry feedstock and enhances ash within the biofuel. Hydrothermal carbonisation (HTC) is an alternative option and involves the processing of wet biomass in hot compressed water (Funke and Ziegler, 2010). It has previously been used as a method to simulate natural coalification in coal petrology but with the emergence of biomass as a future energy source, it now shows potential as a biomass pre-treatment, as it produces a coal like product called hydrochar.

The aim of HTC is to produce a coal like hydrochar which is: (i) more energy dense, (ii) easily friable and (iii) more hydrophobic than the starting material. This is achieved by reducing the oxygen and hydrogen content of the feed (described by the molecular O/C and H/C ratio), destroying the colloidal structures and reducing the hydrophilic functional groups. During HTC, the biomass is submerged in water and is subjected to high temperatures at pressures which prevent the water from evaporating. Under these conditions, water undergoes changes at the molecular level which in turn influence its solvation power, viscosity and polarity (Peterson et al., 2008). As the water is heated and compressed, its density and polarity change reversing its properties from a highly polar hydrogen-bonded solvent to properties more like a non-polar solvent such as hexane (Peterson et al., 2008). Under these conditions, the water provides a medium for a complex series of reactions which involve the removal of hydroxyl groups through dehydration, removal of carboxyl and carbonyl groups though decarboxylation, and cleavage of many ester and ether bonds through hydrolysis (Funke and Ziegler, 2010).

For lignocellulose based biomass, the net result is the macromolecule becoming increasingly aromatised with phenolic structures derived from the dehydration of lignin and aromatisation of carbohydrates derived from the hemicellulose and cellulose. Condensation and polymerisation of the fragments from the main macromolecules also occur, forming humic acid and bitumen based molecules which tend to re-adhere to the hydrochar (Funke and Ziegler, 2010). The detailed nature and the relative significance of the above mechanisms appear strongly dependent on the type and composition of the feed (Funke and Ziegler, 2010). Food waste and microalgae for example have a different biochemical composition (comprising of protein, carbohydrate and lipid) to that of lignocellulosic biomass which comprise of hemicellulose, cellulose and lignin. The proportions of the biochemical components also influence the degradation temperature. For lignocellulosic biomass, hemicellulose appears to degrade first, at temperatures generally below 200° C, cellulose degrades at 200 - 230° C and lignin degrades between 220° C and 260° C (Pastor-Villegas et al., 2006; Libra et al., 2011; Reza et al., 2013). In order to produce a coal like product using hydrothermal processing, a reaction temperature of between 200° C and 250° C is typically used (Funke and Ziegler, 2010). Above 250° C the yield of solid products decrease and give way to a crude oil like product as the conditions favour a process known as hydrothermal liquefaction (HTL). The transition between HTC and HTL appears to be feedstock dependent, with some HTC studies using temperatures above 250°C. Temperature appears to be the most dominant parameter in HTC although the efficiency of the hydrothermal process is also influenced by the percentage of solids in the feed (Libra et al., 2011; Funke and Ziegler, 2010), with increased carbon loss into the water phase with increasing water within the reaction (Libra et al., 2011).

The benefits of the HTC process in terms of combustion are brought about through the low H/C and O/C ratios along with the reduced fraction of volatile matter in the combustible carbon in comparison to the starting biomass. These changes result in increased combustion efficiency, along with reduced pollutant emissions, smoke and water vapour during the combustion process (Liu et al., 2013; Khan et al., 2009). The process has also been shown to influence the ignition temperature and burn out temperatures of the hydrochar, with temperatures increasing with increasing HTC process temperatures, while the activation energy, the critical energy required to start combustion, has been shown to decrease (Parshetti et al., 2013). This can be of particular benefit when blending with low rank coals as it can improve the combustion of low rank coal (Parshetti et al., 2013).

While the handling improvements brought about though HTC are well documented, there has been less research into the fate of inorganic material in the biomass during HTC. Inorganics are a particular issue for biomass during combustion, pyrolysis and gasification as large amounts of alkali and alkaline metals, particularly potassium and sodium, along with sulphur and chlorine influence ash chemistry and influence the behaviours of the fuel in terms of its tendency to corrode equipment and cause slagging and fouling (Koppejan and Van Loo, 2012). The main cause of slagging is attributed to the reactions of alkali metals with silica to form alkali silicates, which melt and soften at temperatures as low as 700° C (Saddawi et al., 2012). The cause of the fouling is attributed to the reaction of the alkali metals with sulphur which form alkali sulphates which can be deposited on heat transfer and combustor surfaces. Chlorine within the ash is very corrosive to stainless steel and can also react with silicates and the alkali metals to form an undesirably stable slag (Masiá et al., 2007). Demineralization of the fuel through dissolution of these alkali salts into the process water during HTC could potentially remove a large fraction of the fuel mineral content thereby reducing the above mentioned ash problems.

Previous work by Saddawi et al., (2012) has demonstrated that simple washing of biomass in distilled water (at room temperature and pressure) can remove simple ionic salts such as alkali earth chlorides which dissolve easily. Washing in solutions such as ammonium acetate can further increase recovery, recovering inorganic elements which are bound to the organic structures of the biomass with ionic bonds, though ion exchange. Finally washing in a hydrochloric acid solution dissolves alkali earth carbonates, sulphates and sulphides. Consecutive leaching using these three methods can subsequently remove the ionic bonded inorganics from the biomass structure, leaving only silicates and elements bound to the organic matrix with covalent bonds (Saddawi et al., 2012). During HTC, the subcritical conditions of water have a lower density and viscosity than that of water under normal conditions (Wagner and Pruß, 2002) and as such, removal of simple ionic salts within the biomass matrix can be enhanced. The increased dielectric content (Archer and Wang, 1990), increased ionic dissociation constant (Bandura and Lvov, 2006) and lower pH (Funke and Ziegler, 2010) of the subcritical water could also aid the removal of ionic bonded inorganics though ion exchange and dissolve the inorganic salts, thus removing ionicly bonded inorganics from the biomass structure. The modification of the biomass structure during HTC will also further aid the removal of the inorganic material.

Reza et al., (2013) investigated the fate of inorganics during HTC for miscanthus, corn stover, switch grass and rice hull. The results have shown reductions in the amount of calcium, sulphur, phosphorus, magnesium and potassium in the original biomass when the biomass is processed under hydrothermal conditions at 200° C, 230° C and 260° C. Removal of silicon appears limited at 200° C and 230° C although there was some indication that silicon content starts to decrease when the lignin starts to degrade at 260° C. It should be noted that despite a decrease in the inorganic content relative to the starting biomass, the overall concentration of inorganics within the char can increase.

In addition to combustion, it has been suggested that HTC derived hydrochars could have other applications in soil amendment or as absorbents for heavy metals due to the high surface chemical functionality (Libra et al., 2011; Hu et al., 2008; Titirici et al., 2007). This investigation has investigated a large number of feedstock including wet biomass wastes such as food waste, anaerobic digestion (AD) press cake, sewage sludge, fibre derived from organically separated municipal wastes and greenhouse waste, a number of terrestrial biomass such as miscanthus, oak and willow and the aquatic biomass: microalgae and macroalgae. The feedstock investigated have a diverse biochemical composition and wide ranging level of inorganics. This work seeks to understand the fate of inorganic material, the production of high energy density biofuels, and following HTC the prediction of fouling behaviour during combustion.

2. Methodology

2.1. Materials

Samples of willow, miscanthus, oak, greenhouse waste, food waste, secondary sewage sludge, AD press cake, macroalgae (Laminaria Hyperborea), microalgae (Chlorella spp.) and fibre derived from municipal waste were used in this investigation. The sample sizes ranged from 1x1 cm to 2x1 cm cuttings for willow and oak, 1x1 cm cuttings for miscanthus, macroalgae, food waste and greenhouse waste, 600-1200 µm for municipal solid waste derived fibre, sewage sludge and AD press cake and a freeze died powder for microalgae. Samples were air dried before treatment and used as received for HTC on the assumption that in an industrial process, HTC would be conducted on chipped fuels to avoid energy-intensive size reduction prior processing taking advantage of the improved grind-ability. For the quantification work a portion of each sample is ground to a size meeting the test requirement.

2.2. Hydrothermal carbonisation

HTC was performed in a 600 ml Parr bench top reactor (Parr, USA) at 200 °C and 250 °C at their isobaric pressures of 16 bar and 40 bar respectfully. The temperature of the reactor was controlled by a PID controller. For each run, 24 g of biomass and 220 ml of distilled water was loaded into the reactor giving approximately 10 % solid loading. The reactor was then heated to the desired temperature at approximately 8 °C minute^{-1} and the reaction temperature held for one hour. After one hour the reactor was allowed to air cool. When cooled, the gas product was released to the atmosphere and the solid and liquid products separated by filtration under gravity using 150 mm qualitative circles (Whatman, UK). The sample was not washed in water or organic solvent. The hydrochar was allowed to air dry in a ventilated fume cupboard for a minimum of 48 hours.

2.3. Analysis

2.3.1. Inorganic analysis

The hydrochar and raw biomass were air dried and homogenised in a Retsch grinder. To determine the inorganic elemental composition (excluding silicon) samples were microwave digested (Aston Parr, USA) with 200 mg of sample in 10 ml concentrated nitric acid (HNO_3). Potassium, sodium, calcium, magnesium and iron were determined by AAS (Valiant, USA), phosphorus and silicon determined using colorimetry and heavy metals determined by ICP-MS (Perkin Elmer, USA). The AAS colorimetric methods was calibrated using standard elemental stock solution (Spectrosol, UK) and two certified biomass reference materials (Elemental Microanalysis, UK) were used to check the calibration and extraction efficiency.

Phosphorus was determined by reacting the acid digested sample with ammonium molybdavanadate solution (0.625 g ammonium matavanadate in 200 ml in 1:1 nitric acid added to 25 grams of ammonium molybdate in 200 ml of deionised water and made up to 500 ml). The colour change was allowed to develop for 30 minutes and measured at 430 nm in a UV-visible photo spectrometer (Thermo Scientific, USA). The silicon content was determined by ashing the biomass and hydrochar samples overnight in a muffle furnace then dissolving 50 mg of ash in a sodium hydroxide melt (1.5 g NaOH). Once cooled, 25 ml of distilled water was added and the sample heated on a steam bath for 30 minutes, the sample was then decanted and thoroughly rinsed into a 600 ml glass beaker and the solution made up to approximately 400 ml with distilled water. 20 ml of 1:1 hydrochloric acid (HCL) is then added and the solution decanted and rinsed into a 1000 ml volumetric flask which is made up to volume using distilled water. 10 ml of solution was then transferred into a 100 ml volumetric flask, diluted to 50-60 ml with distilled water and 1.5 ml of ammonium molybdate solution was added (7.5 g ammonium molybdate, in 75 ml distilled water, followed by 10 ml 1:1 sulphuric acid and finally made up to 100 ml). The solution was allowed to stand for 10 minutes before 4 ml of tartaric acid solution was added (10 g tartaric acid in 100 ml distilled water), followed immediately by 1 ml reducing solution (20 ml 45% sodium hydrogen sulphite solution in 90 ml water, mixed with 0.7 g sodium sulphate and 0.15 g 4-amino 3-hydroxynaphthalene 1-sulphonic acid dissolved in 10 ml distilled water). Solutions were allowed to develop for one hour and the concentration of silicon determined by absorbance at 650 nm in a UV-visible photo spectrometer (Thermo Scientific, USA).

2.3.2. Organic analysis and ash measurement

Carbon, hydrogen, nitrogen and sulphur content of the raw biomass and hydrochar was analysed using a Flash 1112 CHNS analyser (CE Instruments, USA). The instrument was calibrated and checked using calibration standards and certified biomass reference materials (Elemental Microanalysis, UK).

Ash content within the raw biomass and hydrochar was calculated using both ashing in a muffle furnace and using thermo-gravimetric analysis (Mettler Toledo, Switzerland). Oxygen content of the biomass was calculated by difference and higher heating value (HHV) subsequently calculated by Dulong's equation (see equation one).

Equation one: HHV = (0.3383 * % Carbon) + (1.422 * % Hydrogen) – (% Oxygen / 8)

2.3.3. Ash fusion testing

Ash fusion testing (AFT) was performed using a Carbolite digital ash fusion furnace. A digital camera is fixed to the front of the furnace to capture images of the illuminated ash while it is heated from 550 °C to 1570 °C at 7 °C minute^{-1}. The tests were conducted in an oxidising atmosphere with an air flow of 50 ml minute^{-1}. Cylindrical test pieces were formed using dextrin binder (Sigma-Aldrich, USA) and were run in duplicate. Photographs were taken at 5 °C intervals but as the test was performed in accordance with the standard method for the determination of ash melting behaviour (DD CEN/TS 15370-1:2006) stages were given to the nearest 10 °C. The key stage temperatures are as follows: beginning of shrinkage (SST), sample deformation temperature (DT), hemisphere temperature (HT) and flow temperature (FT).

2.3.4. Predictive slagging and fouling indices

To predict the likelihood of fouling during combustion, various slagging and fouling indices have been derived based on the chemical composition of the fuels. The equations for alkali index (AI), bed agglomeration index (BAI), acid base ratio ($R\frac{b}{a}$), slagging (Babcock) index (SI), fouling index (FI), and slag viscosity index (SVI) are given as equations 1-6 in Table 1. For the AI an $AI<0.17$ represents safe combustion, an $AI>0.17<0.34$ predicts probable slagging and fouling and an $AI>0.34$ predicts almost certain slagging and fouling (Jenkins et al., 1998). For BAI, a value of $BAI<0.15$ predicts that bed agglomeration is likely to occur (Bapat et al., 1997). For the $R\frac{b}{a}$ a value of <0.5 indicates a low risk of slagging and an $R\frac{b}{a}>1.0$ predicts a high to severe risk of slagging during biomass combustion. SI values below $SI<0.6$ predict a low slagging inclination, $SI>0.6<2.0$ predicts a medium slagging inclination and $SI>2.0$ predicts a high slagging inclination. For FI values below $FI<0.6$ indicate a low fouling inclination FI>0.6<40.0 medium fouling inclination and FI>40.0 indicate high fouling inclination. An SVI>72 indicates a low slagging indication where SVI>63<72 suggests a medium indication and SIV<65 indicates a high slagging inclination.

2.3.5. Experimental replication and statistical treatment

Analyses were carried out using duplicate samples with errors given within this paper calculated as standard errors. In addition to the analysis of duplicate samples, duplicate analysis by multiple sample injections are performed for most analysis until a maximum standard deviation of ± 2% is achieved. Sampling time for the AAS is automatically increased if the sample deviation within analyte concentration is observed. For colorimetric analysis, a minimum of three separate readings is taken to determine the abortion of the solution, with the abortion taken as the mean figure. For many feedstocks, particularly low ash feedstocks, multiple runs were undertaken in order to obtain an appropriate amount of sample for the analysis, with samples homogenisation performed in a Retsch grinder to minimise sample variation.

3. Results and discussion

3.1. Hydrothermal carbonisation yields

The mass yields of the HTC hydrochars shown in figure 1 are both feedstock and temperature dependant. The yields for the lignocellulosic biomass range between 58 % and 70 % at the lower process temperature (200 °C) and between 40 % and 46 % for the higher process temperature (250 °C). Greenhouse waste, which in this case is largely Paprika waste from Almaria, Spain produces similar yields to lignocellulosics with 59 % and 46 % respectfully. The food waste has a different biochemical composition to that of lignocellulosic material, mainly comprising of protein, carbohydrate and lipid, and has lower yields for both high and low temperature HTC, with 40 % and 44 % respectfully. The smaller difference between the two treatments is linked to the different biochemical content of food waste. The results for the macroalgae and the microalgae, which have a similar biochemical content to the food waste, exhibit a greater reduction in yield compared with food waste with 56 % and 36 % for the macroalgae and 43 % and 28 % for the microalgae at 200 °C and 250 °C respectfully. These yields are significantly lower than for the lignocellulosic based biomasses for both the lower and higher temperature treatments, indicating biochemical composition is an important variable influencing the yield of hydrochar.

For the AD press cake, sewage sludge and to a lesser extent the municipal solid waste (MSW) the high yields are misleading due to the high ash content within the hydrochars. The reduction in yield between the lower and higher temperature treatments for the AD press cake appears to be mostly due to a decrease in the inorganic fraction (ash) within the hydrochar as opposed to greater degradation of the organic fraction. The HTC of AD press cake however results in a significant solubilisation of the organic content into the process water. For sewage sludge, the resultant reduction in yield between 200 and 250° C is due to a combination of both degradation of the organic fraction and removal of inorganic content. For the fibre derived from organically separated municipal wastes, the difference is largely due to degradation of the organic fraction of the hydrochar.

A decrease in ash relative to the starting biomass was observed in all samples, except the fibre derived from organically separated municipal wastes which showed little change, however some caution is needed as the overall concentration of ash within the char can increase. The ash contents of the hydrochars are given in Table 2.

The decrease in yields between the lower and higher temperature treatments is believed to be primarily due to degradation of different biochemical components at the higher temperature. For lignocellulosic based biomass, the significant degradation of cellulose occurring above 210° C (Kumar et al., 2010) explains the higher mass yields at 200°C, with the yield decreasing between 200° C and 250° C due to degradation of the cellulose and to a lesser extent lignin, which begins to degrade between 220° C and 260° C (Pastor-Villegas et al., 2006; Libra et al., 2011; Reza et al., 2013). Increasing the temperature from 200° C to 250° C also increases the pressure from 16 bar to 40 bar, which can exert an influence on the reaction equilibrium. Although this effect has been experimentally shown, it is thought to have a small impact during the HTC process (Funke and Ziegler, 2010).

Reaction time can also influence mass yield. Generally, the mass yield decreases as the reaction time increases. Results from the present HTC experiments together with data from the literature (Sevilla and Fuertes, 2009; Hoekman et al., 2011) suggest that the hydrochar is converted to gaseous and liquid products in the first instance. The increased level of gas production, along with increased char yield with longer residence times could be explained by on-going polymerisation of soluble fragments in the liquid phase which finally lead to precipitation of insoluble solids (Funke and Ziegler, 2010). Kumar et al., (2011) investigated the HTC of organic carbon produced by hydrothermal treatment of switch grass and corn stover. It was observed that soluble oxygenated fragments such as furfural and 5HMF start to disappear with increasing reaction time from 1 h to 4 h. This suggests that these compounds may undergo polymerisation via aldol condensation to form soluble polymers. The aromatic clusters in aqueous solution precipitate as carbon rich microspheres through aromatisation of soluble polymers.

3.2. Ultimate Analysis

The ultimate analysis of the feedstock and hydrochars produced at 200° C and 250° C is listed in Table 2. The ultimate analysis (CHNS) shows an increase in the carbon content (% db) for the hydrochars at 200° C and 250° C compared to the raw feedstock (Table 2). Increased temperatures have been shown to favour higher carbon content, with carbon content increasing in all hydrochars when calculated on a dry ash free basis. Higher HHV is also observed with an increase in temperature. The exception to the rule is the processing of sewage sludge and AD press cake which result in lower HHV due to the large solubilisation of carbon proportional to the ash, although there are still significant increases in carbon density within the organic fraction for both feedstock when calculated on a dry ash free basis. The oxygen content determined by difference showed a significant reduction in all the hydrochars although the oxygen content of the sewage sludge and AD press cake samples maybe underestimated due to the high ash content. The decreased oxygen content is due mainly to decarboxylation and dehydration reactions during HTC. Decarboxylation degrades the carboxyl (-COOH) and carbonyl groups (C=O), forming CO_2 and CO respectively. Dehydration removes hydroxyl groups (-OH) from the feedstock leading to less hydrophilic functional groups. Both reactions can therefore reduce the oxygen content significantly in turn upgrading the energy density. Oxygen loss is of great importance, as its reduction increases the energy content (HHV) of the hydrochars. The reaction temperature also has a clear influence on the reducing oxygen content and increasing carbon content of the hydrochars. 250° C hydrochars contain higher carbon contents when compared to 200° C hydrochars (Table 2). This trend is further supported by the yields of hydrochar shown in Figure 1. Lower yields of hydrochar obtained at 250° C indicate that the decarboxylation and dehydration reactions are more favourable, with significant reductions in the level of oxygen at the higher temperature.

The increase in temperature also has a marked influence on the HHV of the respective hydrochars. The HHV is generally higher for hydrochars produced at 250°C. As discussed previously, the extent of decarboxylation and dehydration is temperature dependent. High temperatures further concentrate the carbon, this coupled with a reduced oxygen content increase the HHV (Table 2). While higher temperatures are associated with lower yields due to a greater amount of organic material undergoing decomposition, the enhanced removal of oxygen offsets this loss in energy terms of energy yield. However the energy yield at 200°C can be higher than hydrochars produced at 250°C due to the higher mass yields obtained at 200°C.

The O/C ratio and the H/C ratio of the hydrochars exhibit lower values when compared to the initial feedstock (Table 2). This will make the fuel more favourable as generally a fuel with low H/C and O/C ratios have reduced energy losses due to smoke and water vapour during the combustion process (Liu et al., 2013). The reduction in the O/C and H/C ratios are a result of removal of CO_2 and H_2O indicating that the hydrochars possess a greater coal like behaviour than the feedstock. This agrees with the literature, which suggests that under hydrothermal conditions, biomass undergoes removal of hydroxyl groups through dehydration, removal of carboxyl and carbonyl groups though decarboxylation, cleavage of ester and ether bonds through hydrolysis and for lignocellulose based biomass, increased aromatisation from the dehydration of lignin and aromatisation of carbohydrates (Funke and Ziegler, 2010).

3.3. Influence of HTC on hydrochar ash chemistry

Table 2 shows the ash content of the raw biomass and the resultant hydrochar on a dry basis. The results have shown that for the lignocellulosic materials and algae, increasing temperature results in a decrease in ash content, while for the organic wastes, the reverse is true. Figure 1 shows the net removal of ash between the 200 °C and 250 °C hydrochars, implying under hydrothermal conditions, a proportion of ash is removed which increases with increasing reaction severity. The reason ash decreases in some hydrochars but increases in others is due to the feedstock specific ash chemistry, with the lignocellulosics having a greater proportion of the inorganic material extracted than organic material, while the organic wastes have a greater proportion of the organic material removed. Thus even though inorganic material is removed, it can still become increasingly concentrated within the hydrochar.

The inorganic concentrations (wt%) within the biomass and the resultant hydrochars also appear to be both element and feedstock dependent. Samples with higher silicon and iron contents appear to result in an increasingly high concentration of ash within the hydrochar, while those without high silicon and iron have a decreasing concentration of ash within the hydrochar. The Major ash forming elements within hydrochars and feedstock are given in table 3 and the net percentage of metal remaining within the hydrochar for potassium (K), sodium (Na), calcium (Ca), magnesium (Mg) and phosphorous (P) is given in table 4. The net percentage of metal remaining within the hydrochar is calculated based on the ratio of inorganic content of the hydrochar with the raw feedstock multiplied by the mass yield at the given temperature. The percentage metal extracted is simply calculated by subtracting the percentage of original metal left within the hydrochar from 100.

Of the main inorganics investigated, potassium (K) and sodium (Na) show the greatest percentage reduction, which is consistent with the leaching experiments undertaken in Saddawi et al., (2012). For potassium, excluding sewage sludge, between 84 % and 97 % of the potassium in the raw biomass was extracted at 250 °C. For HTC at 200 °C removal of potassium was less at between 60 % and 93 %. Sewage sludge had a reduction of approximately 50 % K for both the 200 and 250 °C hydrothermal treatments. This smaller reduction when compared to the other feedstock could be due to the chemical form in which the potassium exists. The potassium reduction is consistent with Reza et al., (2013), which reported reductions in potassium ranging between 80 % and 90 % under hydrothermal conditions at 200, 230 and 260 °C, processing miscanthus, albeit ground to between 600 and 1180 µm. In Saddawi et al., (2012), a washing procedure was used at ambient temperature involving water followed by ammonium acetate and hydrochloric acid resulting in a potassium reduction of 46 % and 62 % for willow and miscanthus respectively compared to the starting biomass using similar sized fuels to this investigation.

Removal of sodium was observed for all samples, with the higher temperature associated with a greater reduction, although the percentage reduction appeared largely dependent on the sodium content of the starting biomass. For willow, miscanthus and oak, reductions of between 46 % and 74 % were observed at 200 °C and reductions of between 64 % and 79 % were observed at 250 °C. The sodium content of the lignocellulosic material is however low in comparison to the other feedstock. Higher sodium containing feedstock, such as AD press cake, food waste, municipal solid wastes, microalgae and macroalgae resulted in far greater sodium removal with between 74 % and 93 % removal at 200 °C and between 87 and 97 % removal at 250 °C. In comparison, Saddawi et al., (2012) reported a 30 % removal of sodium from willow and a 53 % reduction in sodium from miscanthus. Reza et al., (2013) reported reductions in sodium ranging between 31 and 40 % under hydrothermal conditions at 200, 230 and 260 °C, processing ground miscanthus. The sodium content within the miscanthus used in this investigation was similar to that in Saddawi et al., (2012), 177 ppm and 192 ppm respectfully. The sodium content within Reza et al., (2013) was 1451 ppm.

While all the hydrochars have a lower sodium and potassium content than the starting material, the alkaline metals magnesium (Mg) and calcium (Ca) along with phosphorus (P) undergo more limited metal removal. For willow, all three metals are reduced at 200 °C but there is a smaller reduction at 250 °C. For willow, the Mg, Ca and P concentration within the hydrochars is lower than that of the starting biomass but the Mg, Ca and P reduction at 250 °C is almost proportional to the reduction in the organic fraction. The net removal of Mg, Ca and P is also less at 250 °C. This phenomenon is common for the differing feedstock, with only miscanthus, sewage sludge and microalgae having greater removal at 250 °C than 200 °C for Mg, Ca and P. This reduced inorganics removal efficiency is also evident within the results for Reza et al., (2013) which showed the inorganic element yields for miscanthus were substantially lower at 260 °C compared with 200 °C for all elements investigated other than silicon. The reason behind this decrease in metal extraction at higher temperatures could be due to increasing surface functionality of the hydrochars generated at higher temperatures reabsorbing metals from the process waters. It is known that the large number of carboxylic groups on the hydrochar surface which can theoretically increase the cation exchange capacity (CEC) of the hydrochar (Libra et al., 2011). The increased retention of cations could be due to increasing CEC of 250 °C hydrochars. The reduction may also be as a result of reduced extraction efficiency due to an increased build-up of hydrolysis derived products on the outer surface of the biomass macro-molecule at the higher temperature, as is hypothesised in Mosteiro-Romero et al., (2014), reducing the extraction efficiency of the lower solubility salts. Finally there is also evidence that cations can play a role in polymerisation, with studies into the HTC of alginate (structural compound in seaweed) finding that divalent cations, such as calcium and magnesium promote cross linking of alginates oligomers during char formation (Chen et al., 2012). It could be that under the more severe conditions these metals are reincorporated into the hydrochar by this mechanism. While this higher retention of cations in 250 °C hydrochars could be disadvantageous in terms of the final fuel properties of the hydrochar, it could be of benefit if the chars are used in soil amendment.

Calcium extraction appears most efficient in miscanthus with 72 % removed at 200 °C and 89 % removed at 250 °C. Calcium extraction for miscanthus in Reza et al., (2013) was 88 % at 200 °C and 84 % removed at 260 °C. In contest, Saddawi et al., (2012) extracted 19 % of the calcium using their washing technique. In this investigation 66 % of the calcium from willow was removed at 200 °C and 51 % removed at 250 °C, while Saddawi et al., (2012) extracted 3 % of the calcium though biomass washing. For the remaining feedstock investigated calcium varied as shown in table 4 and this resulted in an increase in the calcium content in some of the hydrochars.

Magnesium extraction was most efficient for willow with 75 % extracted at 200 °C and 64 % removed at 250 °C; miscanthus extraction was 60 % and 69 % respectfully. Reza et al., (2013) extracted 88 % magnesium from miscanthus at 200 and 250 °C. Saddawi et al., (2012) extracted 14 % magnesium from willow and 56 % magnesium from miscanthus using biomass washing. For the remaining feedstock in this study (excluding sewage sludge) between 33 % and 71 % magnesium was extracted at 200 °C and between 33 % and 67 % magnesium was extracted at 250

°C. For the lignocellulosic biomass and greenhouse wastes a net reduction in magnesium within the char was observed while for the remaining feedstock, magnesium became more concentrated within the char.

Phosphorous extraction followed similar trends to that of calcium and magnesium with the highest extractions associated with willow, miscanthus and microalgae. Phosphorous extraction for willow was 72 % and 68 %; miscanthus was 50 % and 70 %; and microalgae 60 % and 76 % for 200 °C and 250 °C respectively. Reza et al., (2013) extracted 90 % phosphorous from miscanthus at 200 °C and 58 % at 250 °C. Saddawi et al., (2012) extracted 56 % phosphorus from willow and 49 % magnesium from miscanthus using biomass washing.

For most biomass materials, the major element speciation can be divided into three categories: (i) water soluble ionic salts, (ii) organically associated metals ionic or covalently bonded with tissue, and (iii) amorphous, crystalline or pure precipitated compounds (Korbee et al., 2001; Marschner and Marschner, 2012). Most of the sodium and potassium within the biomass is in the form of ionic salts (>90%) such as sodium nitrate, sodium chloride, potassium nitrate and potassium chloride. For magnesium, between 60 and 90 % is in the form of ionic salts comprising of magnesium nitrate, chloride and phosphate, with a large proportion of the remainder being organically associated with chlorophyll and the biomass macromolecule. For calcium, between 20 and 60 % is in the form of nitrate, chloride and phosphate ionic salts; a small proportion is incorporated into the biomass macromolecule, and the remainder is in the form of amorphous or crystalline compounds. Phosphorus occurs in both its ionic form and organically associated in protein, phospholipids and nucleic acids (Korbee et al., 2001; Marschner and Marschner, 2012). The type of compound in which the metal is associated within the biomass is likely to strongly influence the extraction efficiency during HTC. A large proportion of potassium and sodium within the biomass is in the form of soluble ionic salts and this corresponds to a larger extraction of these metals. The magnesium, calcium and phosphorus is less easily extracted and corresponds to its association with organic matter in the biomass.

Limited leaching of silicon, titanium, iron and aluminium have been reported under hydrothermal conditions in Reza et al., (2013) and several biomass washing experiments (Deng et al., 2013;

Werkelin et al., 2010; Miles et al., 1995) using finely ground biomass, however due to their very low solubility (Miles et al., 1995) and the larger particle size used in these experiments it is assumed there was only limited removal.

3.4. Influence of HTC on ash behaviour during combustion

The concentrations of the major ash forming elements within biofuels are listed in table 3 and it is the behaviour of these elements within the ash which is often a critical factor in commercial furnaces, such as those used in steam power generation. The main issue with ash is the potential for it to slag and foul within the furnace which can lead to reduced thermal efficiency, corrosion and difficulties associated with removal of ash from the furnace. As most furnaces are designed to remove ash as a powdery residue, it is undesirable for an ash to become sticky or worse melt. If the ash becomes sticky or fuses into a hard glassy slag, known as a clinker, it makes extraction difficult and the furnace requires cleaning. High temperatures are advantageous as they can increase the thermal efficiency of the furnace and reduce the formation of oxides of nitrogen (NO_x) which form from fuel bound nitrogen at temperatures between 800 °C and 1100 °C (Koppejan and Van Loo, 2012).

The temperature at which the ash melts and fuses is strongly influenced by the alkali and alkaline metals which act as a flux for alumina-silicate ash (Koppejan and Van Loo, 2012). Generally speaking calcium and magnesium increase the melting temperatures of ashes while potassium and sodium decrease it, although due to complex interactions between potassium, chlorine, sulphur, silicon and calcium each element cannot always be evaluated individually (Koppejan and Van Loo, 2012). Table 5 contains the ‘deformation’ temperature, the point the ash starts to become sticky and potentially problematic, and the ‘flow’ temperature, the temperature in which it melts, for the ash fusion results for the raw feedstock and hydrochars as defined in DD CEN/TS 15370-1:2006: Method for determination of ash melting behaviour. Figures 2a-d give the transition temperatures between phases defined in DD CEN/TS 15370-1:2006 for willow, miscanthus, macroalgae and microalgae feedstock. The results show that HTC has a strong influence on the ash fusion temperatures with the processed fuels becoming sticky (deformation) and melting (flow) at higher temperatures than the raw feedstock. This finding would support the theory that a large proportion of the potassium and sodium within the starting biomass is removed following HTC, reducing the flux effect they have on ash melting. The more limited removal of magnesium and calcium under HTC, especially at 250 °C has been shown to result in increased concentrations of magnesium and calcium in the hydrochar. This could be advantageous as the change in alkali to alkaline ratio within the char should increase the melting /fusion temperature.

Slagging potential is largely determined though fusion temperatures, with a decrease in fusion temperature indicating an increase in slagging potential (Koppejan and Van Loo, 2012). The increase in fusion temperatures observed via the HTC consequently indicates slagging potential is reduced by HTC, with greater reductions brought about at higher temperatures. Table 5 contains the results of a number of predictive slagging indices used to evaluate the influence of the ash chemistry, with their equations given in Table 1. These indices are based on the chemical composition of the biomass and ranks the ash in terms of its propensity to form fused slag deposits (Koppejan and Van Loo, 2012). HTC appears to result in a net improvement in the slagging indices with the Alkali Index (AI) improving for all feedstock, as it increases the calorific value of the fuel while reducing the potassium and sodium content. The limited removal of iron (Fe) under HTC, resulting in its accumulation within the char, resulting in improvements in bed agglomeration index (BAI), slag viscosity index (SVI) and base to acid ratio (R b/a). Some of the biomass however is predicted to have high slagging propensities, for example willow when calculated using BAI, SVI and R b/a predict high slagging propensity due to low silicon and titanium dioxide, despite high fusion temperatures outside of the furnace range (furnace limit 1570 °C).

Some caution is needed when interpreting chemical composition based slagging indices as these indices are based on coal ash slagging and assume the ashes will behave like alumino-silicate coal ashes. Biomass ash systems are chemically very different to alumino-silicate coal and care is needed when comparing conventional slagging index values for biomass (Koppejan and Van Loo, 2012). This could explain the results for macroalgae, despite the 250 °C hydrochar having a flow temperature greater than that of the furnace limit, which suggests a low slagging potential (see figure 2c), all slagging indices, indicate a high slagging inclination. The results could also be due to the form the potassium takes in the fuel which may not be volatilised under these conditions. The presence of alginate, a carbohydrate consisting of alginic acid associated with an inorganic salt, within the algae cell wall, means that the chemistry of algae is slightly different to that of the other feedstock used in this research. Due to the thermal stability of the alginate it is likely that some of the alginate will have remained in the ash (Ross et al., 2011) and this would have influenced how potassium and sodium behaves the ash. While previous reports of high slagging seaweeds in Ross et al., (2008) appear to be verified, it appears that hydrothermally processes seaweeds may perform significantly better. The low transition temperatures for microalgae could be due to the low silicon content within the feedstock. Strain selection could yield significantly higher transition temperatures.

In addition to slagging, fouling is another major issue in commercial furnaces. Fouling is brought about when potassium and sodium, in combination with chlorine, partially evaporate during the combustion process and form alkali chlorides which condense on the heat exchanger surfaces. These deposits don't just reduce the heat exchanger efficiency; they also play a major role in corrosion as these deposits react with sulphur in the flue gas to form alkali sulphates releasing chlorine in the process. This chlorine has a catalytic effect which results in the active oxidation and corrosion of the furnace material (Koppejan and Van Loo, 2012). HTC has been shown to reduce the potassium and sodium within the hydrochar which based on the AI, reducing the risk of fouling. It has also been suggested that HTC reduces fouling risk through the combination of decreased oxygen and volatile matter content of the hydrochars (Liu et al., 2013) which can potentially reduce the release of inorganic vapours during combustion (Khan et al., 2009). HTC should also reduce the chlorine within the fuel. Chlorine exists within biomass in the form of water soluble ionic salts (NaCl, KCl, $CaCl_2$, $MgCl_2$ and ionic chloride (Cl^-)) (Korbee et al., 2001; Marschner and Marschner, 2012) with the ionic salts making up a large proportion of the total inorganics extracted under HTC. The extraction of these chloride based salts will result in the extracted chlorine appearing as chloride in the process waters. Biomass washing experiments have shown that between 85 % and 100 % of total chlorine within the biomass is extracted though washing (Deng et al., 2013; Saddawi et al., 2012; Miles et al., 1995). The fouling inclination calculated by the Fouling Index (FI) was shown to improve after HTC however a number of feedstock and hydrochar were calculated as having high fouling inclination due to low silicon and titanium dioxide in the fuel.

4. Conclusions

It can be concluded that the hydrochar yields for lignocellulosics typically range from between 58 % and 70 % at the lower process temperature (200 °C) and between 40 % and 46 % for the higher process temperature (250 °C). The yields for the non-lignocellulosic materials such as sewage sludge, AD presscake and algae were significantly lower than for the lignocellulosic based biomasses for both the lower and higher temperature treatments indicating that biochemical composition has a significant impact on hydrochar yield. The lower yields of hydrochar obtained at 250° C indicate that the decarboxylation and dehydration reactions are more favourable, with significant reductions in the level of oxygen at the higher temperature. These decarboxylation and dehydration reactions subsequently increase the energy content (HHV) of the hydrochars.

This study has shown that a large proportion of the potassium and sodium within the feedstock is extracted during HTC, while magnesium and calcium along with phosphorus undergo more limited removal. The removal of these metals has a significant influence on the slagging and fouling propensity of the fuel, demonstrating the importance of metal removal in terms of the combustion behaviour of the resultant fuel. The results show that treatment of biomass by HTC has a strong influence on the slagging propensity of the fuel, with ash fusion temperatures for the processed fuels melting at higher temperatures to that of the raw feedstock. This research demonstrates that HTC can produce a coal like hydrochar from a range of feedstock which is: (i) more energy dense, (ii) easily friable and (iii) more hydrophobic than the starting material, it also could overcome the issues of slagging and fouling associated with the starting material.

5. Acknowledgements

The authors would like to thank the EPSRC Doctoral Training Centre in Low Carbon Technologies (EP/G036608/1) for financial support of Aidan Smith and the European

Commission for financial support of the ‘Biorefine’ project via the ERDF Interreg IVb NWE region programme for partial support of the research. The authors would also like to thank Graphite Resources, UK for supply of fibre derived from municipal solid waste and Mr Simon Lloyd and Dr Adrian Cunliffe for their technical assistance.

6. References

Archer, D. G. & Wang, P. (1990). The Dielectric Constant of Water and Debye-Hückel Limiting Law Slopes. Journal of physical and chemical reference data, 19**,** 371-411.

Bandura, A. V. & Lvov, S. N. (2006). The ionization constant of water over wide ranges of temperature and density. Journal of Physical and Chemical Reference Data, 35**,** 15-30.

Bapat, D., Kulkarni, S. & Bhandarkar, V. 1997. Design and operating experience on fluidized bed boiler burning biomass fuels with high alkali ash. American Society of Mechanical Engineers, New York, NY (United States).

Chen, J., Chen, Z., Wang, C. & Li, X. (2012). Calcium-assisted hydrothermal carbonization of an alginate for the production of carbon microspheres with unique surface nanopores. Materials Letters, 67**,** 365-368.

Deng, L., Zhang, T. & Che, D. (2013). Effect of water washing on fuel properties, pyrolysis and combustion characteristics, and ash fusibility of biomass. Fuel Processing Technology, 106**,** 712-720.

Funke, A. & Ziegler, F. (2010). Hydrothermal carbonization of biomass: A summary and discussion of chemical mechanisms for process engineering. Biofuels, Bioproducts and Biorefining, 4**,** 160-177.

Hoekman, S. K., Broch, A. & Robbins, C. (2011). Hydrothermal carbonization (HTC) of lignocellulosic biomass. Energy and Fuels, 25**,** 1802-1810.

Hu, B., Yu, S.-H., Wang, K., Liu, L. & Xu, X.-W. (2008). Functional carbonaceous materials from hydrothermal carbonization of biomass: an effective chemical process. Dalton Transactions**,** 5414-5423.

Ibrahim, R. H. H., Darvell, L. I., Jones, J. M. & Williams, A. (2013). Physicochemical characterisation of torrefied biomass. Journal of Analytical and Applied Pyrolysis, 103**,** 21-30.

Jenkins, B., Baxter, L. & Miles, T. (1998). Combustion properties of biomass. Fuel processing technology, 54**,** 17-46.

Khan, A. A., de Jong, W., Jansens, P. J. & Spliethoff, H. (2009). Biomass combustion in fluidized bed boilers: Potential problems and remedies. Fuel Processing Technology, 90**,** 21-50.

Koppejan, J. & Van Loo, S. 2012. The handbook of biomass combustion and co-firing, Routledge.

Korbee, R., Kiel, J., Zevenhoven, M., Skrifvars, B., Jensen, P. & Frandsen, F. (2001). Investigation of biomass inorganic matter by advanced fuel analysis and conversion experiments. Proc. Power Production in the 21st Century: Impacts of Fuel Quality and Operations. United Engineering Foundation Advanced Combustion Engineering Research Center. Snowbird UT., Oct.

Kumar, S., Gupta, R., Lee, Y. Y. & Gupta, R. B. (2010). Cellulose pretreatment in subcritical water: Effect of temperature on molecular structure and enzymatic reactivity. Bioresource Technology, 101**,** 1337-1347.

Kumar, S., Kothari, U., Kong, L., Lee, Y. Y. & Gupta, R. B. (2011). Hydrothermal pretreatment of switchgrass and corn stover for production of ethanol and carbon microspheres. Biomass and Bioenergy, 35**,** 956-968.

Libra, J. A., Ro, K. S., Kammann, C., Funke, A., Berge, N. D., Neubauer, Y., Titirici, M. M., Fühner, C., Bens, O., Kern, J. & Emmerich, K. H. (2011). Hydrothermal carbonization of biomass residuals: A comparative review of the chemistry, processes and applications of wet and dry pyrolysis. Biofuels, 2**,** 71-106.

Liu, Z., Quek, A., Kent Hoekman, S. & Balasubramanian, R. (2013). Production of solid biochar fuel from waste biomass by hydrothermal carbonization. Fuel, 103**,** 943-949.

Marschner, H. & Marschner, P. 2012. Marschner's mineral nutrition of higher plants, Academic press.

Masiá, A. T., Buhre, B., Gupta, R. & Wall, T. (2007). Characterising ash of biomass and waste. Fuel Processing Technology, 88**,** 1071-1081.

Miles, T. R., Miles Jr, T., Baxter, L., Bryers, R., Jenkins, B. & Oden, L. 1995. Alkali deposits found in biomass power plants: A preliminary investigation of their extent and nature. Volume 1. National Renewable Energy Lab., Golden, CO (United States); Miles (Thomas R.), Portland, OR (United States); Sandia National Labs., Livermore, CA (United States); Foster Wheeler Development Corp., Livingston, NJ (United States); California Univ., Davis, CA (United States); Bureau of Mines, Albany, OR (United States). Albany Research Center.

Mosteiro-Romero, M., Vogel, F. & Wokaun, A. (2014). Liquefaction of wood in hot compressed water: Part 1—Experimental results. Chemical Engineering Science, 109**,** 111-122.

Parshetti, G. K., Kent Hoekman, S. & Balasubramanian, R. (2013). Chemical, structural and combustion characteristics of carbonaceous products obtained by hydrothermal carbonization of palm empty fruit bunches. Bioresource Technology, 135**,** 683-689.

Pastor-Villegas, J., Pastor-Valle, J. F., Rodríguez, J. M. M. & García, M. G. (2006). Study of commercial wood charcoals for the preparation of carbon adsorbents. Journal of Analytical and Applied Pyrolysis, 76**,** 103-108.

Peterson, A. A., Vogel, F., Lachance, R. P., Fröling, M., Antal Jr, M. J. & Tester, J. W. (2008). Thermochemical biofuel production in hydrothermal media: a review of sub- and supercritical water technologies. Energy & Environmental Science, 1**,** 32-65.

Reza, M. T., Lynam, J. G., Uddin, M. H. & Coronella, C. J. (2013). Hydrothermal carbonization: Fate of inorganics. Biomass and Bioenergy, 49**,** 86-94.

Ross, A. B., Hall, C., Anastasakis, K., Westwood, A., Jones, J. M. & Crewe, R. J. (2011). Influence of cation on the pyrolysis and oxidation of alginates. Journal of Analytical and Applied Pyrolysis, 91**,** 344-351.

Ross, A. B., Jones, J. M., Kubacki, M. L. & Bridgeman, T. (2008). Classification of macroalgae as fuel and its thermochemical behaviour. Bioresource Technology, 99**,** 6494-6504.

Saddawi, A., Jones, J. M., Williams, A. & Le Coeur, C. (2012). Commodity fuels from biomass through pretreatment and torrefaction: Effects of mineral content on torrefied fuel characteristics and quality. Energy and Fuels, 26**,** 6466-6474.

Sevilla, M. & Fuertes, A. B. (2009). The production of carbon materials by hydrothermal carbonization of cellulose. Carbon, 47**,** 2281-2289.

Titirici, M.-M., Thomas, A. & Antonietti, M. (2007). Back in the black: hydrothermal carbonization of plant material as an efficient chemical process to treat the CO 2 problem? New Journal of Chemistry, 31**,** 787-789.

Wagner, W. & Pruß, A. (2002). The IAPWS formulation 1995 for the thermodynamic properties of ordinary water substance for general and scientific use. Journal of Physical and Chemical Reference Data, 31**,** 387-535.

Werkelin, J., Skrifvars, B.-J., Zevenhoven, M., Holmbom, B. & Hupa, M. (2010). Chemical forms of ash-forming elements in woody biomass fuels. Fuel, 89**,** 481-493.

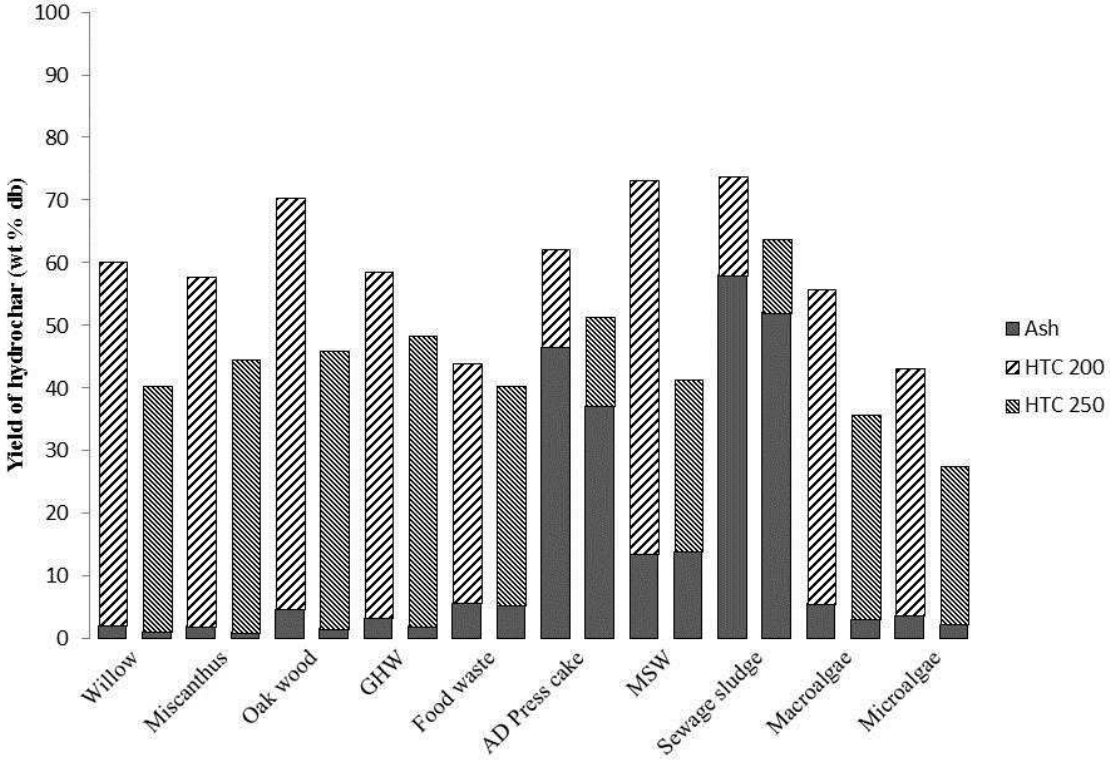

Figure 1: Hydrochar mass yields under hydrothermal conditions at 200° C and 250° C respectfully.

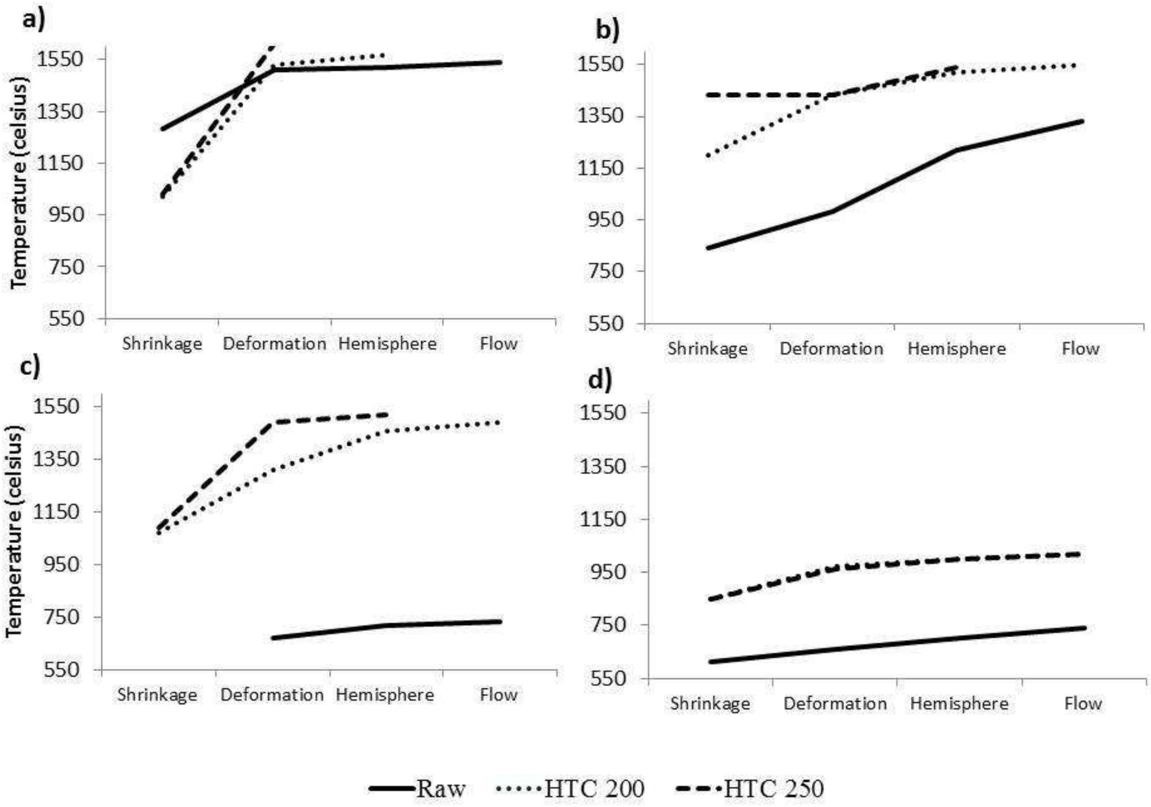

Figure 2: Ash fusion transition temperatures for a) willow, b) miscanthus, c) macroalgae and d) microalgae.

Table 1: Predictive slagging and fouling indices

Slagging/fouling index	Expression	Limit
Alkali Index	$AI = \frac{Kg\ (K_2O + Na_2O)}{GJ}$	AI<0.17 safe combustion AI>0.17<0.34 probable slagging and fouling AI>0.34 almost certain slagging and fouling
Bed Agglomeration Index	$BAI = \frac{\%(Fe_2O_3)}{\%(K_2O + Na_2O)}$	BAI<0.15 bed agglomeration likely
Acid Base Ratio	$R_{\frac{b}{a}} = \frac{\%(Fe_2O_3 + CaO + MgO + K_2O + Na_2O)}{\%(SiO_2 + TiO_2 + Al_2O_3)}$	R$_{\frac{b}{a}}$ <0.5 low slagging risk
Slagging Index	$SI = (\frac{\%(Fe_2O_3+CaO+MgO+K_2O+Na_2O)}{\%(SiO_2+TiO_2+Al_2O_3)}$)*%S(dry)	SI<0.6 low slagging inclination SI>0.6<2.0 medium slagging inclination SI>2.0 high slagging inclination
Fouling Index	$FI = (\frac{\%(Fe_2O_3+CaO+MgO+K_2O+Na_2O)}{\%(SiO_2+TiO_2+Al_2O_3)}$)* $\%(K_2O + Na_2O)$	FI<0.6 low fouling FI>0.6<40.0 medium fouling FI>40.0 indicate high fouling
Slag Viscosity Index	$SVI = \frac{(\%\ SiO_2 * 100)}{\%(SiO_2 + MgO + CaO + Fe_2O_3)}$	SVI>72 low slagging indication SVI>63<72 medium slagging indication SIV<65 high slagging inclination

Table 2: Ultimate analysis results for feedstock and hydrochars

Feedstock	% C (db)	% H (db)	% N (db)	%S (db)	% O (db)	HHV (MJ/kg)	% Ash (db)	H/C (daf)	O/C (daf)	Energy Yield (%)
Willow	45.3±0.2	6.2±0.3	0.5±0.0	0.1±0.0	43.8	16.4	4.1	1.64	0.73	-
HTC 200	58.9±0.6	7.2±0.1	1.4±0.0	0.2±0.0	29.0	25.0	3.5	1.47	0.37	92.0
HTC 250	70.4±0.0	5.3±0.1	1.3±0.0	0.1±0.0	20.2	27.8	2.7	0.90	0.22	44.7
Miscanthus	46.0±0.0	5.7±0.1	0.5±0.0	0.1±0.0	42.8	16.1	4.9	1.49	0.70	-
HTC 200	61.1±0.6	6.2±0.1	0.8±0.0	0.1±0.0	28.3	24.5	3.5	1.22	0.35	88.0
HTC 250	71.0±0.6	7.9±0.0	1.1±0.0	0.2±0.0	17.5	32.1	2.3	1.34	0.18	58.5
Oak Wood	43.4±0.5	5.9±0.1	0.3±0.1	0.1±0.1	42.9	15.4	7.4	1.63	0.74	-
HTC 200	55.0±0.1	4.6±0.1	1.0±0.0	0.0±0.0	32.7	19.3	6.7	1.00	0.45	88.1
HTC 250	72.2±0.6	6.6±0.0	2.2±0.0	0.2±0.0	15.2	31.1	3.6	1.10	0.16	71.8
Greenhouse waste	45.7±2.6	6.7±0.3	1.1±0.5	0.2±0.0	36.4	18.5	9.9	1.76	0.60	-
HTC 200	59.6±0.1	6.3±0.1	1.9±0.0	0.0±0.0	26.5	24.4	5.7	1.27	0.33	77.8
HTC 250	68.5±0.1	6.1±0.1	3.6±0.0	0.2±0.0	17.4	28.8	4.2	1.07	0.19	54.3
Foodwaste	46.7±0.4	7.6±0.2	2.9±0.0	0.1±0.1	28.0	21.6	7.1	1.95	0.45	-
HTC 200	54.8±1.1	7.0±0.2	1.1±0.1	0.2±0.0	24.1	24.2	12.9	1.53	0.33	49.3
HTC 250	62.8±2.1	6.9±0.3	1.3±0.2	0.2±0.0	15.4	28.3	13.5	1.32	0.18	47.2
AD press cake	17.8±1.3	2.3±0.1	0.3±0.0	0.0±0.1	12.1	8.8	63.9	1.55	0.62	-
HTC 200	14.0±0.4	1.4±0.2	0.5±0.0	0.1±0.1	9.3	9.1	74.8	1.20	0.50	25.7
HTC 250	22.5±0.1	1.8±0.0	0.7±0.0	0.0±0.0	7.1	7.7	72.2	0.23	0.33	30.0
Municipal wastes	38.8±0.5	5.8±0.1	1.3±0.0	0.0±0.0	19.8	17.9	28.3	1.79	0.38	-
HTC 200	38.8±0.1	5.2±0.1	1.1±0.0	0.1±0.0	36.3	14.1	18.6	1.61	0.70	57.7
HTC 250	50.0±0.2	6.3±0.1	2.7±0.0	0.1±0.0	7.2	24.6	33.7	1.51	0.11	56.9
Sewage sludge	13.1±0.4	3.7±0.2	4.1±0.1	2.4±0.0	13.7	7.3	63.0	3.38	0.78	-
HTC 200	13.2±0.4	1.8±0.1	1.1±0.0	0.1±0.0	5.2	6.0	78.7	1.61	0.29	61.4
HTC 250	11.6±0.4	1.3±0.2	0.9±0.0	0.1±0.1	4.6	5.0	81.5	1.37	0.30	52.8
Macroalgae	31.6±0.1	5.2±0.0	2.8±0.0	4.5±0.0	35.3	11.8	20.6	1.97	0.84	-
HTC 200	48.2±0.2	4.7±0.2	2.3±0.0	0.1±0.1	34.5	16.8	10.2	1.17	0.54	79.6
HTC 250	59.5±1.7	5.4±0.3	5.9±0.1	0.1±0.0	20.5	24.6	8.6	1.09	0.26	52.9
Microalgae	48.4±0.3	7.2±0.1	7.8±0.1	0.3±0.0	27.1	21.8	9.2	1.79	0.42	-
HTC 200	58.0±0.3	7.0±0.0	5.3±0.0	0.0±0.0	20.8	25.8	8.8	1.44	0.27	51.1
HTC 250	62.1±0.1	6.8±0.1	4.8±0.0	0.0±0.0	17.9	27.5	8.4	1.32	0.22	29.2

Table 3: Major ash forming elements within hydrochars and feedstock

Feedstock	Na (wt%)	Mg (wt%)	P (wt%)	K (wt%)	Ca (wt%)	Fe (wt%)	Si (wt%)	S (wt%)
Willow	0.01	0.12	0.05	0.28	0.20	0.01	0.03	0.10
HTC 200	0.01	0.05	0.02	0.07	0.11	0.01	0.01	0.16
HTC 250	0.01	0.11	0.08	0.11	0.24	0.01	0.02	0.10
Miscanthus	0.02	0.06	0.02	0.17	0.20	0.01	2.10	0.10
HTC 200	0.01	0.04	0.02	0.08	0.09	0.01	2.81	0.10
HTC 250	0.01	0.04	0.01	0.05	0.05	0.01	2.91	0.21
Oak Wood	0.01	0.08	0.02	0.16	2.37	0.01	0.02	0.02
HTC 200	0.01	0.06	0.01	0.07	3.25	0.01	0.08	0.01
HTC 250	0.01	0.07	0.03	0.06	2.67	0.02	-	0.21
Greenhouse waste	0.04	0.81	0.08	4.03	1.58	0.01	0.20	0.24
HTC 200	0.03	0.57	0.06	2.58	2.44	0.02	0.15	0.02
HTC 250	0.02	0.61	0.16	0.51	1.34	0.08	0.10	0.19
Foodwaste	0.73	0.11	0.12	0.76	1.58	0.04	0.50	0.09
HTC 200	0.11	0.07	0.15	0.12	0.85	0.22	1.37	0.15
HTC 250	0.07	0.18	0.26	0.05	2.78	0.13	1.19	0.15
AD press cake	0.19	0.59	0.17	0.87	1.92	0.82	52.70	0.00
HTC 200	0.04	0.50	0.14	0.35	1.56	0.88	-	0.00
HTC 250	0.03	0.93	0.18	0.22	2.18	0.96	47.22	0.00
Municipal wastes	0.54	0.54	0.09	0.53	3.84	0.60	10.19	0.50
HTC 200	0.19	0.50	0.09	0.26	3.34	0.57	7.69	0.10
HTC 250	0.05	0.88	0.17	0.15	2.45	0.86	15.92	0.11
Sewage sludge	0.10	0.65	0.28	0.89	1.73	3.33	33.24	2.42
HTC 200	0.04	0.81	0.35	0.64	2.28	4.14	48.17	2.86
HTC 250	0.04	0.86	0.23	0.69	2.26	4.29	42.21	
Macroalgae	2.44	0.72	0.08	4.38	0.73	0.01	0.16	4.51
HTC 200	1.06	0.48	0.11	1.91	0.96	0.03	0.13	3.95
HTC 250	0.91	0.81	0.19	1.63	1.46	0.04	0.10	2.96
Microalgae	0.31	0.45	0.44	0.50	0.76	0.03	0.34	3.03
HTC 200	0.10	0.70	0.41	0.16	1.53	0.06	0.31	3.09
HTC 250	0.05	0.98	0.38	0.07	1.75	0.05	0.36	2.59

Table 4: The percentage of potassium, sodium, calcium, magnesium and phosphorous remaining within the hydrochar after hydrothermal processing

Feedstock	Na (wt%)	Mg (wt%)	P (wt%)	K (wt%)	Ca (wt%)
Willow	-	-	-	-	-
HTC 200	54	25	28	16	34
HTC 250	36	36	59	16	49
Miscanthus	-	-	-	-	-
HTC 200	26	41	50	29	28
HTC 250	21	31	30	12	11
Oak Wood	-	-	-	-	-
HTC 200	54	50	57	31	97
HTC 250	30	37	82	16	52
Greenhouse waste	-	-	-	-	-
HTC 200	48	44	41	40	91
HTC 250	22	26	67	4	30
Foodwaste	-	-	-	-	-
HTC 200	7	29	53	7	14
HTC 250	4	64	85	3	42
AD press cake	-	-	-	-	-
HTC 200	14	49	52	24	51
HTC 250	7	76	56	12	58
Municipal wastes	-	-	-	-	-
HTC 200	26	67	71	36	64
HTC 250	3	67	77	12	26
Sewage sludge	-	-	-	-	-
HTC 200	29	92	92	53	97
HTC 250	26	83	53	50	83
Macroalgae	-	-	-	-	-
HTC 200	24	37	76	24	73
HTC 250	13	41	88	13	71
Microalgae	-	-	-	-	-
HTC 200	14	67	40	14	86
HTC 250	5	60	24	4	63

Table 5: Fouling indices and ash fusibility flow temperature

Feedstock	**Fouling and Slagging Indices**						**Ash Behaviour (°C)**	
	AI	**BAI**	**R b/a**	**SI**	**FI**	**SVI**	**Deformation**	**Flow**
Willow	0.16	0.03	2.1	0.2	39.4	6	1310±0	1540±0
HTC 200	0.04	0.11	0.6	0.1	9.9	4	1330±10	>1570
HTC 250	0.05	0.14	1	0.1	25.4	3	>1570	>1570
Miscanthus	0.11	0.06	0.3	0	1.7	84	980±10	1350±20
HTC 200	0.04	0.13	0.1	0	0.3	93	1430±0	1550±0
HTC 250	0.02	0.27	0.1	0	0.1	95	1430±0	>1570
Oak Wood	0.08	0.07	66.6	1.3	445	1	1390±0	1420±0
HTC 200	0.03	0.15	80.5	0.8	127	1	1360±10	1410±0
HTC 250	0.02	0.33	1.3	0.3	1.6	43	1480±0	1520±0
Greenhouse waste	2.45	0	2.1	0.5	94	6	1480±10	1550±0
HTC 200	1.28	0.01	37.8	0.8	1933	3	1410±0	1480±0
HTC 250	0.22	0.19	47	8.9	718	1	1500±0	1540±0
Foodwaste	0.71	0.03	7.2	0.7	180	18	1570±0	>1570
HTC 200	0.1	1.05	2.9	0.4	17.8	24	1450±10	>1570
HTC 250	0.04	1.2	5.1	0.8	10.4	13	1420±20	1530±0
AD press cake	1.14	0.9	0.1	0	0.2	92	1330±20	1430±10
HTC 200	0.95	2.62	3.2	0	2.1	0	1320±10	1530±10
HTC 250	0.3	4.65	0.1	0	0	89	1420±20	1550±20
Municipal wastes	0.66	0.63	0.6	0.3	2.9	59	1150±0	1200±0
HTC 200	0.4	1.43	0.6	0.1	1.8	55	1160±0	1190±0
HTC 250	0.1	5.01	0.3	0	0.2	73	1180±0	1240±0
Sewage sludge	1.71	3.95	0.3	0.6	0.5	80	1230±0	1430±0
HTC 200	1.67	7.2	0.2	0.6	0.2	82	1220±0	1440±0
HTC 250	0.88	6.93	0.2	0	0.3	80	1240±0	1470±0
Macroalgae	9.49	0	16.2	73.2	1526	5	670±0	730±0
HTC 200	2.03	0.01	11.1	44.1	412	5	1310±0	1490±0
HTC 250	1.28	0.02	14.1	41.8	523	4	1490±0	>1570
Microalgae	0.43	0.04	4.1	12.4	45.4	15	660±0	740±0
HTC 200	0.11	0.27	4.8	14.9	18.9	8	970±0	1020±0
HTC 250	0.07	0.5	4.9	12.8	6	8	1180±0	1020±0